NPS-58Bb75021

NAVAL POSTGRADUATE SCHOOL
Monterey, California

A HIGH FREQUENCY PLATINUM RESISTANCE THERMOMETER

SYSTEM FOR MEASURING

TURBULENT ATMOSPHERIC TEMPERATURE FLUCTUATIONS

Noel E. J. Boston and Edman L. Sipe

February 1975

Technical Report for Period 1 July 74 - 1 February 75

Approved for public release; distribution unlimited

Prepared for:
Chief of Naval Research
Arlington, Virginia 22217

NAVAL POSTGRADUATE SCHOOL
Monterey, California

Rear Admiral Isham Linder   Jack R. Borsting
Superintendent   Provost

REPORT DOCUMENTATION PAGE		READ INSTRUCTIONS BEFORE COMPLETING FORM
1. REPORT NUMBER NPS-58Bb75021	**2. GOVT ACCESSION NO.**	**3. RECIPIENT'S CATALOG NUMBER**
4. TITLE *(and Subtitle)* A HIGH FREQUENCY PLATINUM RESISTANCE THERMOMETER SYSTEM FOR MEASURING TURBULENT ATMOSPHERIC TEMPERATURE FLUCTUATIONS		**5. TYPE OF REPORT & PERIOD COVERED** TECHNICAL REPORT 1 July 74 – 1 Feb 75 **6. PERFORMING ORG. REPORT NUMBER**
7. AUTHOR(s) Noel E. J. Boston Edman L. Sipe		**8. CONTRACT OR GRANT NUMBER(s)**
9. PERFORMING ORGANIZATION NAME AND ADDRESS Naval Postgraduate School Monterey, California 93940		**10. PROGRAM ELEMENT, PROJECT, TASK AREA & WORK UNIT NUMBERS** 61153N: RR131-03-01: NR 083-275: WR-5-0020
11. CONTROLLING OFFICE NAME AND ADDRESS Chief of Naval Research Arlington, Virginia 22217		**12. REPORT DATE** February 1975 **13. NUMBER OF PAGES**
14. MONITORING AGENCY NAME & ADDRESS *(If different from Controlling Office)*		**15. SECURITY CLASS.** *(of this report)* Unclassified **15a. DECLASSIFICATION/DOWNGRADING SCHEDULE**

16. DISTRIBUTION STATEMENT *(of this Report)*

Approved for public release; distribution unlimited

17. DISTRIBUTION STATEMENT *(of the abstract entered in Block 20, if different from Report)*

18. SUPPLEMENTARY NOTES

19. KEY WORDS *(Continue on reverse side if necessary and identify by block number)*

turbulence
atmospheric temperature fluctuations
platinum resistance thermometer

20. ABSTRACT *(Continue on reverse side if necessary and identify by block number)*

A sensor and electronic system has been developed and used to measure high frequency, small scale atmospheric temperature fluctuations.

The sensor consists of a platinum wire $0.25\mu m$ in diameter and $0.30mm$ in length. The wire has a time constant of less than $10\mu sec$ in a 4 m/sec air flow. With a detection current of 50μ amps its sensitivity is 0.063 mv/$^{\circ}$C.

The electronic system consists of an 80kHz multivibrator, bridge,

DD FORM _{1 JAN 73} **1473** EDITION OF 1 NOV 65 IS OBSOLETE
S/N 0102-014-6601 |

bridge amplifier, synchronous detector and DC amplifier. The overall system frequency response is flat from DC to 4.5 kHz. The bridge has a noise level of 0.40µv rms and is capable of measuring temperature changes of $0.048^{\circ}C$. The overall system noise level varied from 0.18 mv at 10 Hz to 1.6 mv at 1 kHz. Methods are suggested for improving these figures.

<u>List of Figures</u>

A HIGH FREQUENCY PLATINUM RESISTANCE THERMOMETER SYSTEM
FOR MEASURING TURBULENT ATMOSPHERIC TEMPERATURE FLUCTUATIONS

A High Frequency Platinum Resistance Thermometer System
For Measuring Turbulent Atmospheric Temperature Fluctuations

Noel E. J. Boston and Edman L. Sipe
Department of Oceanography, Naval Postgraduate School
Monterey, California 93940

ABSTRACT

A sensor and electronic system has been developed and used to measure high frequency, small scale atmospheric temperature fluctuations.

The sensor consists of a platinum wire 0.25 μm in diameter and 0.30 mm in length. The wire has a time constant of less than 10 μsec in a 4 m/sec air flow. With a detection current of 50 μamps its sensitivity is 0.063 mv/$^{\circ}$C.

The electronic system consists of an 80 kHz multivibrator, bridge, bridge amplifier, synchronous detector and DC amplifier. The overall system frequency response is flat from DC to 4.5 kHz. The bridge has a noise level of 0.40 μv rms and is capable of measuring temperature changes of 0.048°C. The overall system noise level varied from 0.18 mv at 10 Hz to 1.6 mv at 1 kHz. Methods are suggested for improving these figures.

1. Introduction

The measurement of temperature fluctuations in the atmosphere is conceptually not difficult, however to measure temperature fluctuations at frequencies much greater than 10 Hz presents several practical difficulties. The sensor must be small, and as a result very fragile, to explore the scales of interest yet it must operate in exposed atmospheric conditions. The level of the temperature fluctuations beyond 10 Hz is often small which means operating with small electrical signals. Finally, because of the sporadic nature of small scale turbulence, a rather wide dynamic range is required of the detection system.

There are several problem areas which make the construction of a low noise, high frequency atmospheric temperature measuring system an honourable task. First, there are those problems associated with basic turbulence research: the shape of the high wave-number temperature spectrum, the evaluation of the scalar constant (?) which appears in the expression for the universal -5/3 form of the temperature spectrum, the higher moments of passive scalars. Second, there are those problems associated with boundary layer meteorology: heat fluxes, similarity theory, . microthermals. And third, there are those problems associated with very applied problems such as laser, radio wave and acoustic transmission in the atmosphere.

The system that will be described here is not considered to be a 100% satisfactory solution to the problem of measuring high frequency atmospheric temperature fluctuations. It achieves admirable success in some quarters and marginal success on others. These will become clear and indeed emphasized in the test. The system then is not considered to be an end product and suggestions for improvement are included. Its main advantages at present are 1) it is available and 2) it has been used successfully.

4

2. The Sensor

a. Dimensions

The sensor consists of a platinum wire 0.25 μm (.00001 inches) in diameter and 0.30 mm in length. These dimensions, besides being important to frequency response and wave-number resolution, have particular significance with respect to the electronic system. These aspects will be discussed in turn.

In order to obtain information on temperature fluctuations in the atmosphere to the very smallest scales it is now clear from a number of studies that temperature fluctuations in excess of 1000 Hz must be measured. For purposes of design it is prudent to assume that somewhat higher frequencies may be encountered, such as up to 3000 Hz. At a wind speed of 6 m/sec the spatial scale associated with such frequencies is 2 mm. Since the minimum scale the wire is able to resolve is twice its length then its spatial resolution is not in doubt. In fact if only the one-dimensional temperature spectrum is considered and the wire length is perpendicular to the flow direction it is able to resolve much finer temperature structure in the downstream direction.

The transient response of resistance wire thermometers has received considerable attention over the years. However, it is the work of Chao and Sandborn (1964) which is particularly applicable to this study. They examined in detail the transient behaviour of a 90% platinum -10% rhodium wire whose dimensions were .63 μm (.000025 inches) in diameter and 1.6 mm in length. They measured the frequency response of the wire and found it to be 3200 Hz in still air, increasing to 4600 Hz in air moving at 6 m/sec. Because of the similarity of the dimensions and physical properties of the wire used in their study and in this it seems reasonable to extrapolate by simple ratios their results to this case. The frequency response is inversely proportional to the square of the diameter

5

and (more or less) to the length of the wire. The wire used here being 2.5

times smaller in diameter and one-fifth as long should have a frequency response

in excess of 140 kHz. Since non-linearities are ignored in such scaling it is

perhaps safer to put the frequency response at 100 kHz, which means a time

constant of 10 μsec. Calculations based on expressions developed by Fabula (1962)

and Krechmer (1954) lead to similar results. Clearly, the frequency response

of this wire exceeds by almost two orders of magnitude the already generous anti-

cipated requirements.

b. Construction

The sensor was made from Wollastin wire consisting of a silver jacket

about a platinum core. The outside diameter of the jacket is about 45 μm (.0018

inches). The original wire (jacket and core) was prestressed into a V-shape

and then soldered onto the end of a standard hot-wire anemometer probe (Figure 1)

in such a way that when the silver jacket was removed there was no undue stress

on the thin platinum core. The silver jacket was electro-chemically removed by

placing the wire in a bubble of dilute nitric acid at the drawn tip of a U-tube

(Figure 2) and applying 1.5 v DC. The jacket flakes off exposing the platinum

core (Figure 3). With some skill and much practice sensors of lengths varying

from 0.25 mm to 0.50 mm may be made. No special devices (such as comparators

or lathe benches) are required to perform this task with the exception of a 100

power microscope and a firm surface upon which to rest shaky hands.

3. The Bridge

a. Design

The measurement of temperature fluctuations with a thin platinum wire

takes advantage of the fact that a very slightly heated wire is a simple resis-

tance thermometer. The wire is necessarily slightly heated by a small current

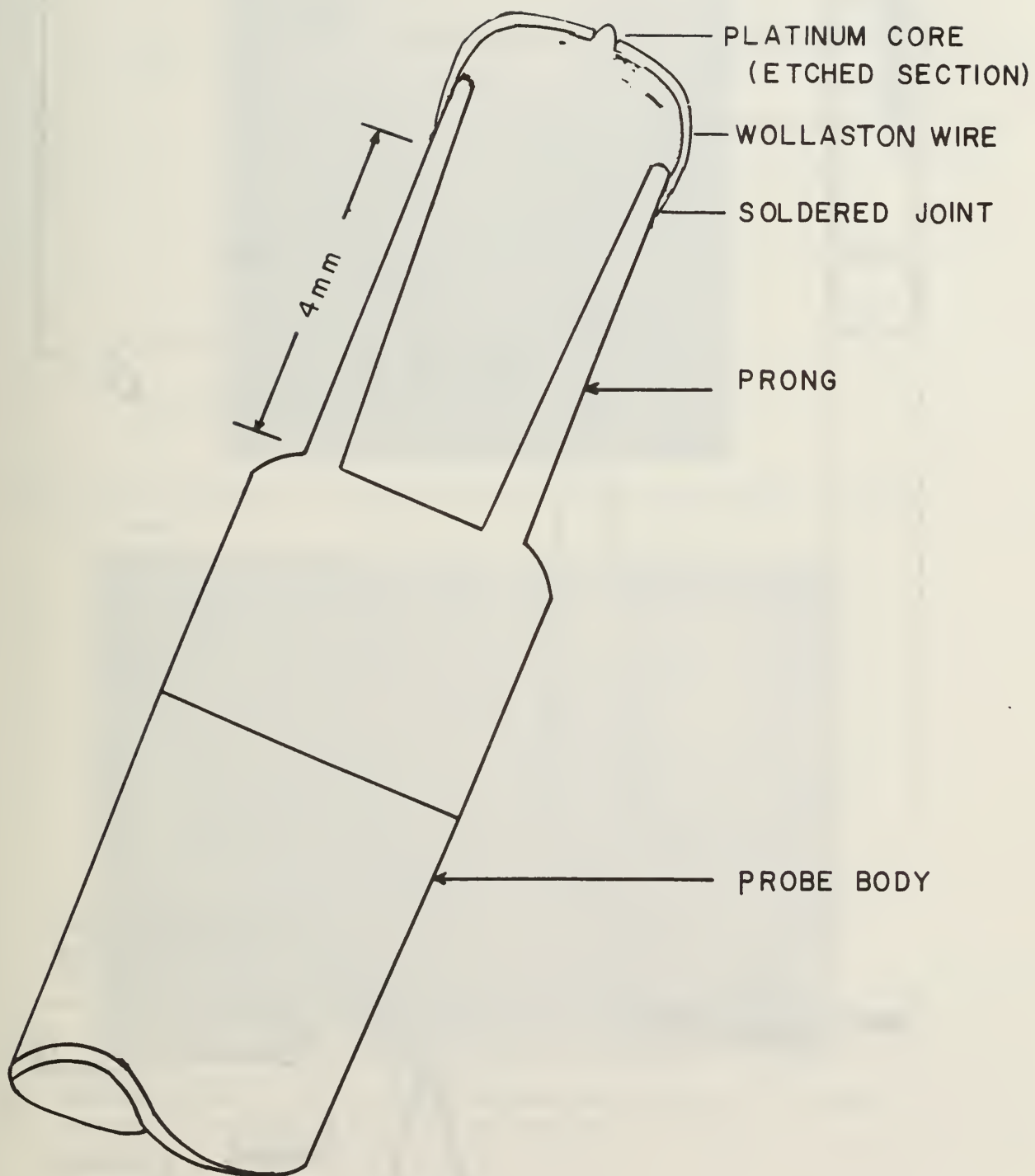Figure 1. "Wollaston" Wire Mounted on Probe .

7
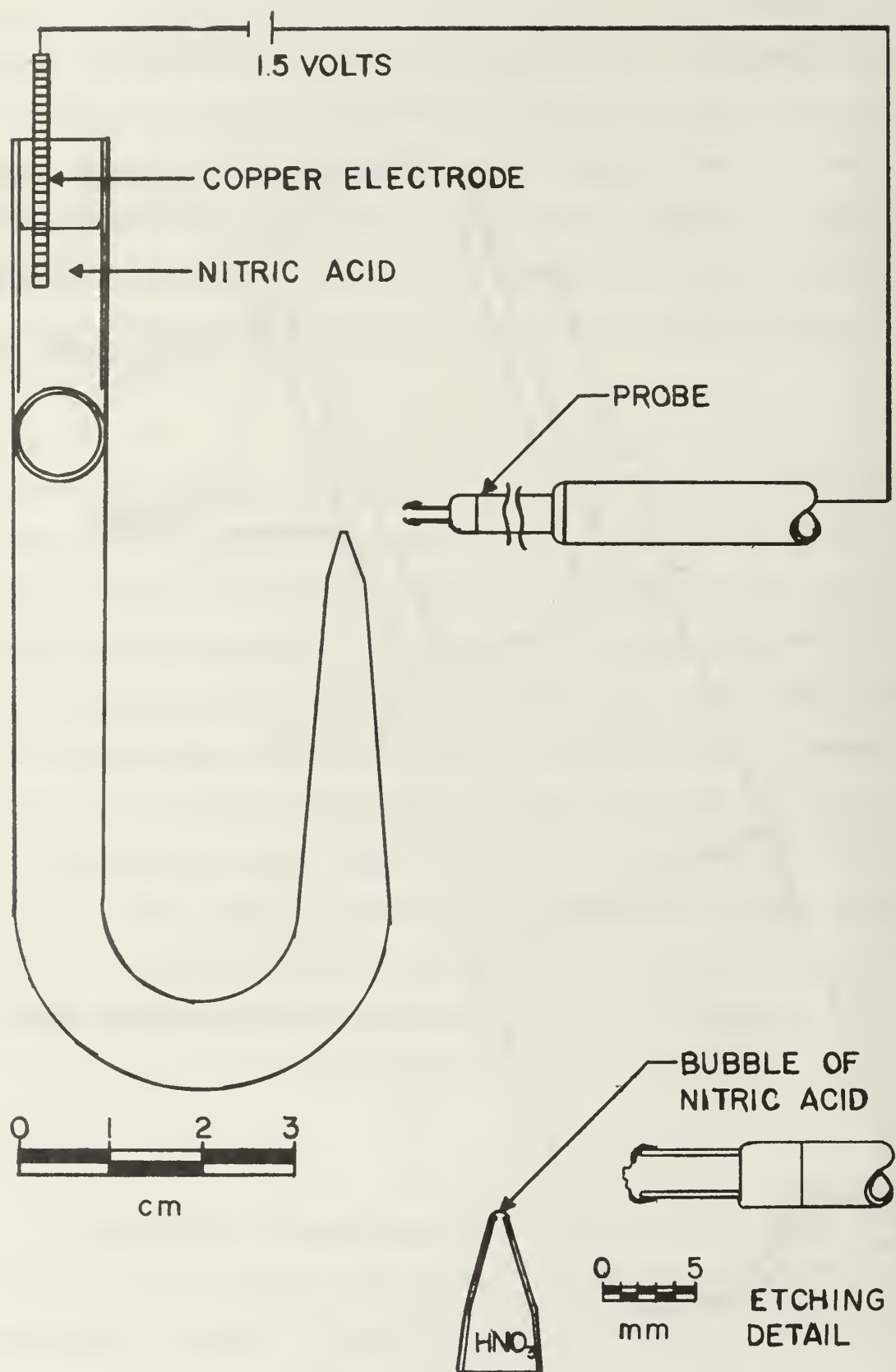
Figure 2. The Etching Procedure.

8

(a) 0.25 μm platinum wire core extending from silver jacket soldered to prongs.

(b) Magnification of (a) to show platinum core section. Distance between silver coated ends is approximately 0.4 mm.

Figure 3. Microscope photographs of platinum core used as the temperature fluctuation sensor. Photographs by Charles Woodhouse.

in order to sense its change in resistance due to change in ambient temperature
by measuring the change in voltage across it. If this heating is kept low, re-
sistance changes due to cooling by the wind are negligible compared to resistance
changes cuased by temperature variations. The bridge design then consists essen-
tially of calculating values of bridge resistors to ensure optimum current
through the wire.

The rate at which heat is transferred from a cylinder (wire) to an air
stream in steady flow has been found by King (1914) to be proportional to the
square root of velocity. In this application his result reduces to the propor-
tionality

$$H \ \alpha \ L\Delta T \ \sqrt{Ud} + constant \tag{1}$$

where H is the rate of heat transfer to the air stream L is the length of the
wire, U is the mean wind speed and d is the diameter of the wire. ΔT is the
overheat of the wire and is defined as

$$\Delta T = T_w - T_e \tag{2}$$

with T_w being the wire temperature and T_e the equilibrium temperature of the
unheated wire. If the resistance of the wire is R ohms and it carries a cur-
rent of I amperes then the rate at which electrical energy is converted into
heat in the wire is I^2R watts. In steady flow the rate of heat loss is equal to
the rate at which heat is supplied to the wire, or

$$H = I^2R \ \ \alpha L\Delta T \ \sqrt{Ud} + constant . \tag{3}$$

This expression, after suitable rearrangement, allows one to plot ΔT as a
function of U for given values of I. The object is to select I such that the
velocity induced change in ΔT is small compared with the effect of ambient
temperature fluctuations for a typical range of velocities.

The optimum value of the current through the 0.25 μm wire chosen was
determined experimentally. The probe was connected to a bridge (Figure 4)
and the sensor placed in a small wind tunnel. A measured voltage was applied
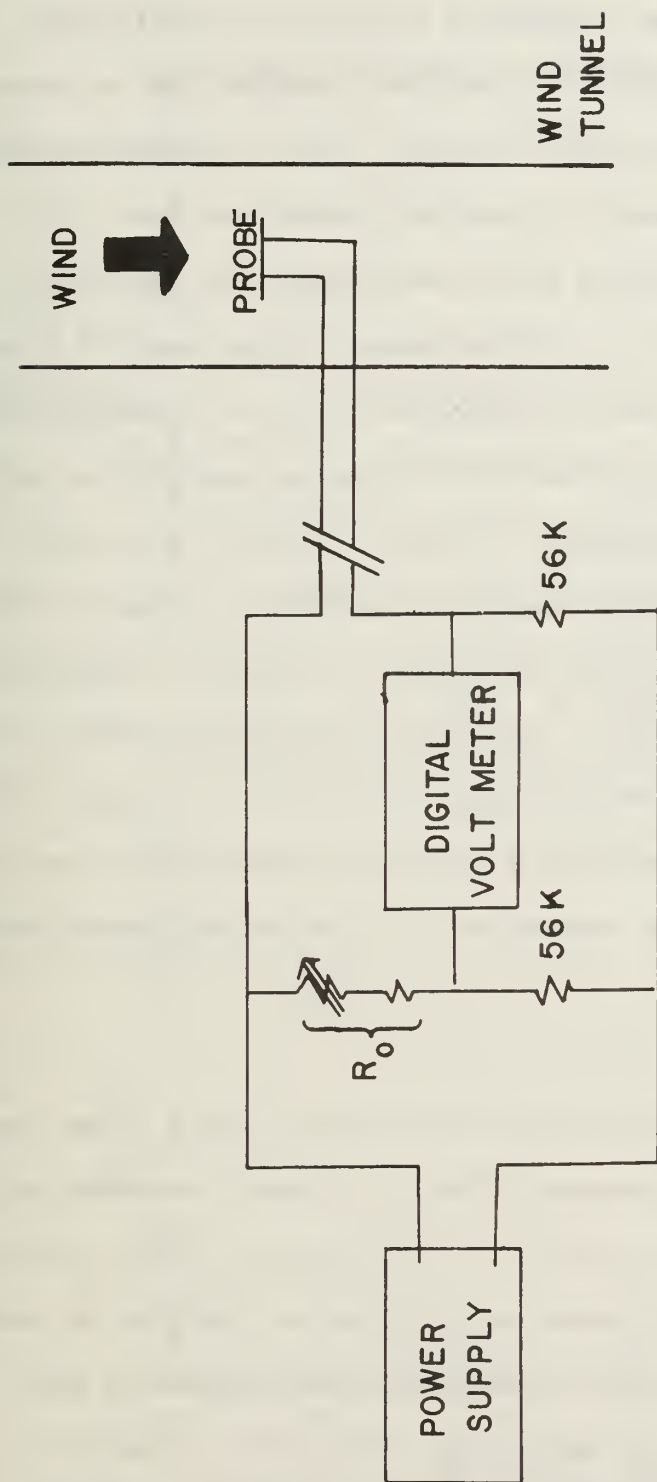
Figure 4. Circuit Used to Test Response of Platinum Resistance Thermometer to Wind Speed.

11

to the bridge and the output voltage recorded as a function of wind speed. The current through the wire was calculated and over-heat computed from an exact form of Eq. (3) [from Flow Corporation Bulletin #25, 1956]; this was plotted against (mean wind speed)$^{1/2}$ in Figure 5. When the current was about 100 microamps through the wire, the velocity effect was larger than desirable (approximately equivalent to $0.03C°$ per 1 m/sec change in wind speed at 4 to 5 m/sec). In order to be certain that no significant velocity dependence appeared in the temperature signal the 0.25 μm diameter wire was operated with a current of 50 microamps. A change in wind speed of 4 m/sec to 5 m/sec, for example, would be registered as a temperature change of only 0.005°C. Wyngaard (1971) has pointed out that velocity sensitivity which may be completely negligible for the computation of reliable spectra, can cause the measured skewness of the temperature derivative to be large and positive. The results of Boston (1973a) although supporting Wyngaard indicate that the system discussed here comes very close to being sufficiently velocity insensitive to allow accurate measurements of temperature derivative skewness.

b. Calibration

An indirect method was used to calibrate the sensor and bridge combination because static and dynamic methods proved to be very unsatisfactory. A 2.5 μm diameter platinum wire was placed in a low dielectric fluid, calibrated and the calibration compared with a theoretical calibration based on the physical properties of the platinum. The assumption was made that if there is good agreement between the results, then a theoretical calibration of the 0.25 μm diameter wire, which was not strong enough to penetrate the surface of the fluid, should be adequate.
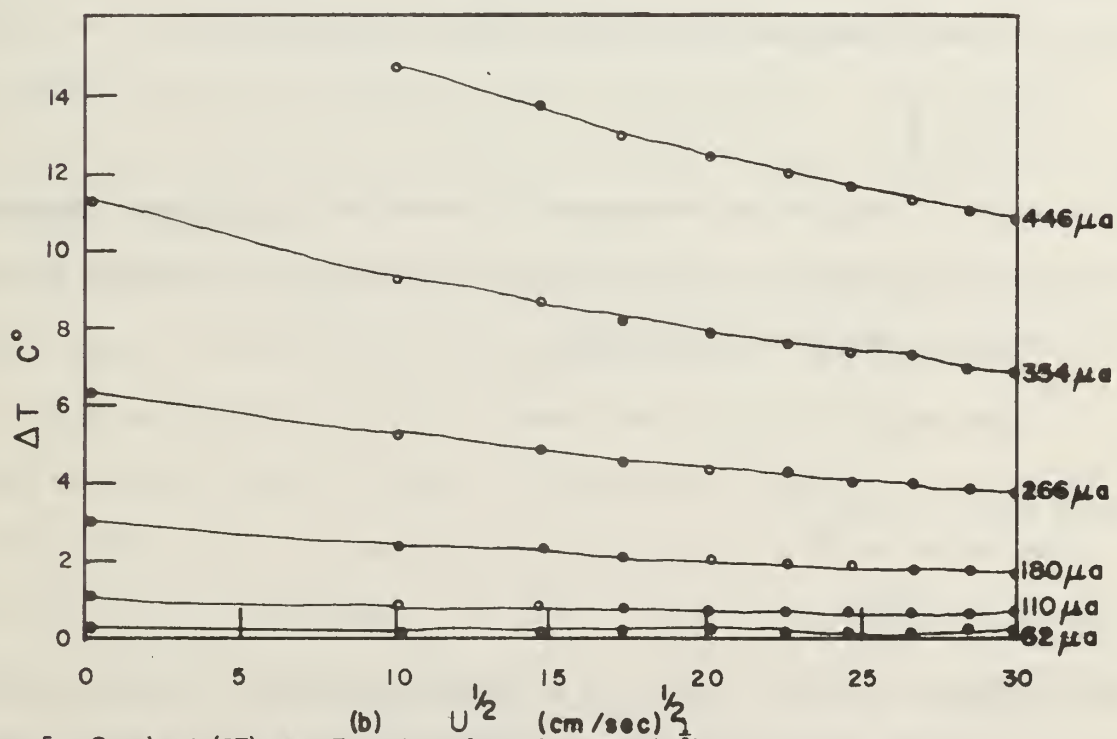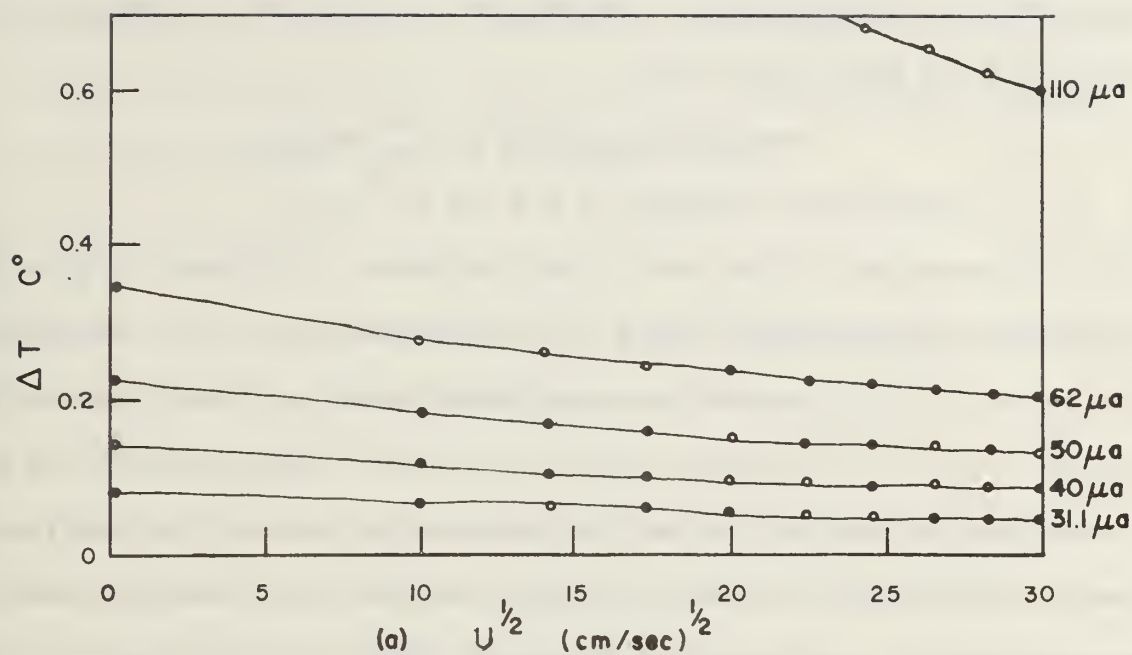
12

Figure 5. Overheat (ΔT) as a Function of Wind Speed (U^2) for Various Currents through Platinum Wire Sensor.

13

The resistivity and temperature coefficient of the wires were assumed to be those of bulk platinum. The Handbook of Chemistry and Physics (45th edition) lists these values as:

$$\text{resistivity } \rho_o = 11 \times 10^{-6} \text{ ohm-cm,}$$
$$\text{temperature coefficient } \alpha = 3.7 \times 10^{-3} \text{ (C}^\circ)^{-1}.$$

The resistance of the core of the "Wollaston" wire used, as given by the manufacturer (Sigmund Cohn Corp.), is 6,000 ohms per foot (20 ohms/mm) for the coarse (2.5 μm diameter) wire and 600,000 ohms per foot (2,000 ohm/mm) for the fine (0.25 μm diameter) wire. The etched length is about 3.0 mm for the coarse wire and 0.30 mm for the fine wire which means the resistance of the coarse wire is about 60 ohms and that of the fine wire about 600 ohms. This agrees reasonably well with the resistance (R) as obtained from the resistivity (ρ_o) and the dimensions of the wire (length ℓ and area A):

$$R = \rho_o \frac{\ell}{A} . \tag{4}$$

The range of temperature encountered in atmospheric turbulence measurements is small so the change in resistivity can be assumed to be linearly proportional to change of temperature according to

$$\Delta\rho = \rho_o \alpha \Delta T \tag{5}$$

From Eqs. (4) and (5)

$$\Delta R = \left(\frac{\rho_o \alpha \ell}{A}\right) \Delta T \tag{6}$$

The bracketed term has a value of 0.249 for the coarse wire and 2.49 for the fine wire. This is the change in resistance in ohms for each wire for a one C° temperature change.

A resistance box was substituted for the sensor in the bridge which then was balanced for typical sensor resistances (600 Ω to 900 Ω). At balance a

14

change in the resistance box of one ohm with the D.C. amplifier (section 3e) of the platinum resistance thermometer electronics set at a gain of 20 resulted in a D.C. voltage level change of 0.4 volts, or $\Delta V/\Delta R = 0.4$ volts/ohm. Since, from the preceding paragraph, $\Delta R/\Delta T = 2.5$ ohms/C° then

$$\frac{\Delta V}{\Delta R} \cdot \frac{\Delta R}{\Delta T} = 1 \text{ volt/C°} \tag{7}$$

at a gain of 20. With the D.C. amplifier at a gain of 10 a voltage change of one volt corresponded to a temperature change of 0.5 C°.

c. Circuit details

The details of the bridge circuit (Figure 6) may now be described. It is a modified Wheatstone bridge consisting of two 2.21 KΩ resistors, sensor, probe and cable, balance adjustment resistors and capacitors. The balance resistance may be varied from 500 Ω to 1000 Ω by the series combination of a 200 Ω variable resistor and one or more selectable fixed resistors. The fixed and variable capacitors paralleling the balance resistance are necessary to match the probe and cable capacitance.

The linearity of the bridge was checked by substituting a dummy probe in place of the sensor and probe upon which it was mounted. Four sensor resistance values between 500 Ω and 1000 Ω were chosen arbitrarily as points about which linearity would be tested. The dummy probe was set to one of the values, the bridge output voltage balanced to zero and the dummy probe then changed by 1/2 Ω to 2 Ω increments. For the four cases the output voltage was measured as a function of bridge unbalance. The results (Figure 7) showed that the output voltage varied linearly with bridge unbalance. The credit for linearity is in part due to the high input impedance of the differential amplifier (Figure 6) which allows the bridge output voltage to remain linear over a wide range. Further, these results indicate that the differential and operational amplifiers also were linear and not saturated by a sensor resistance change equivalent to a 6°C temperature change. A minor drawback is that
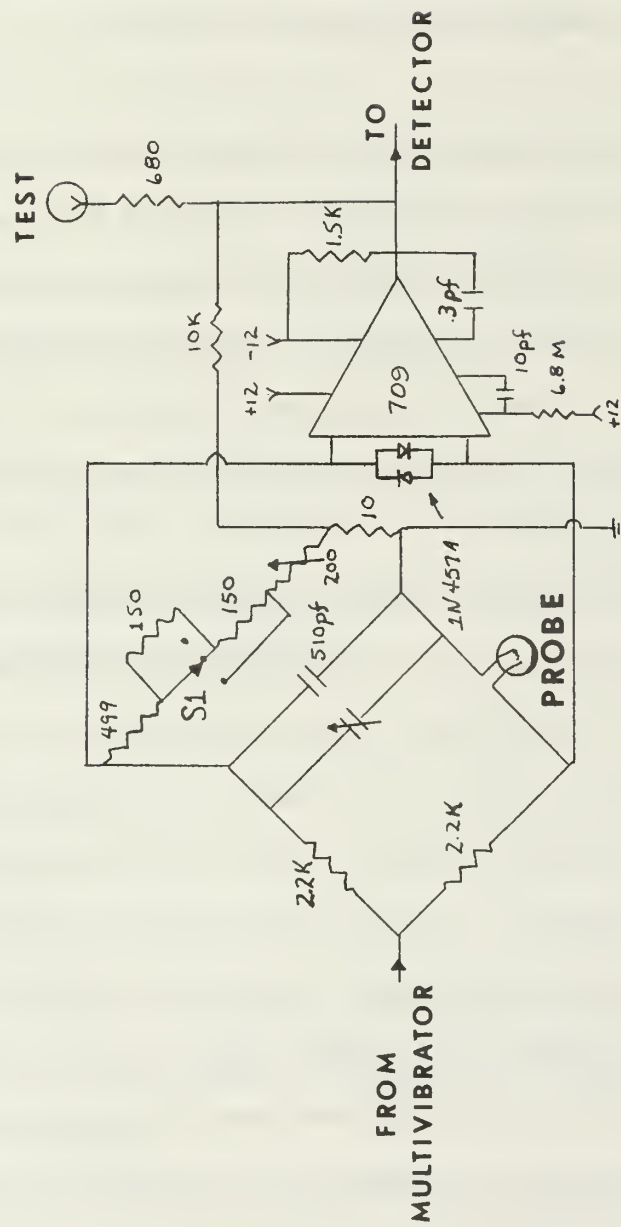
15

Figure 6. Bridge Circuit and Bridge Differential Amplifier.
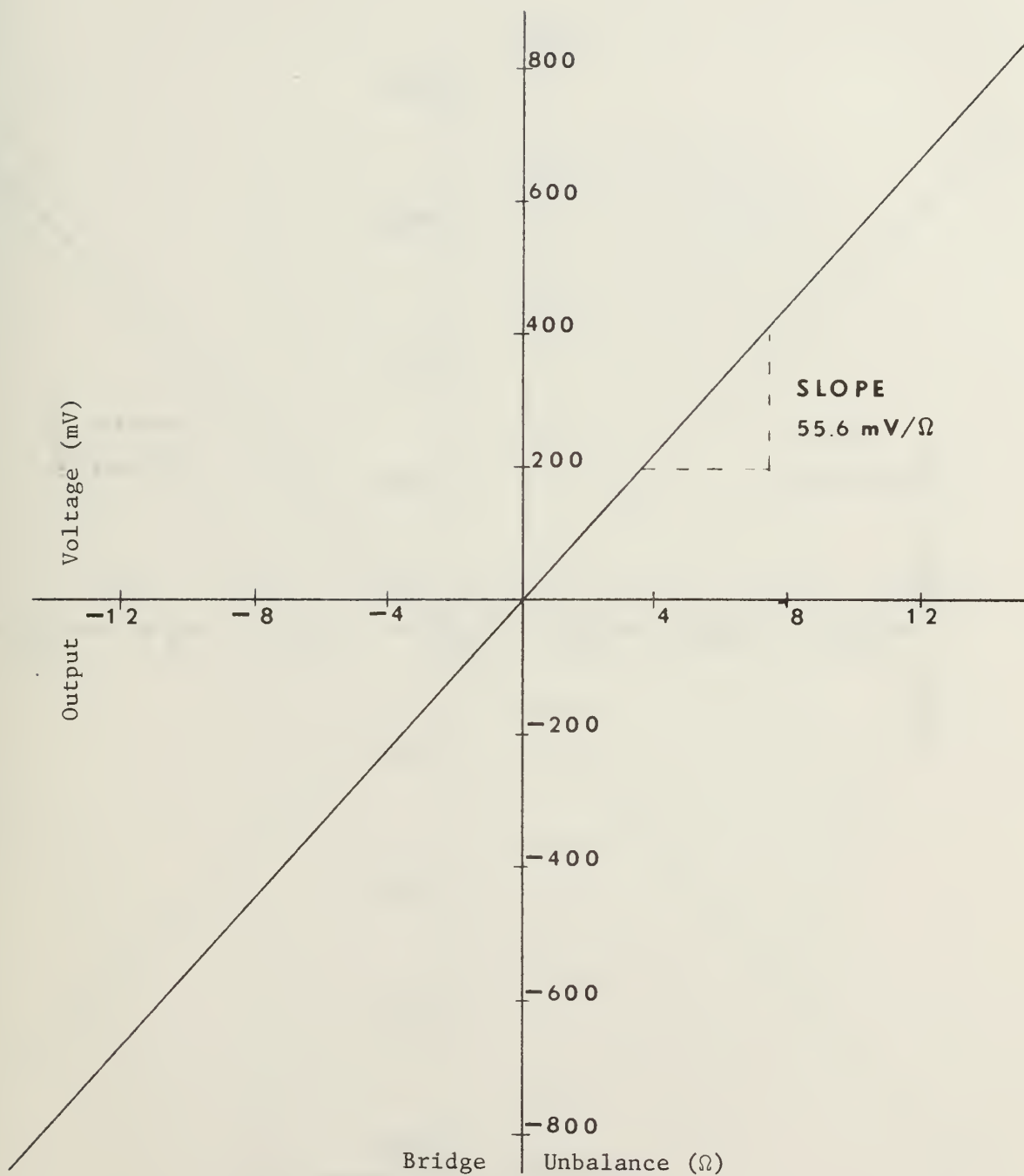
16

Figure 7a.   Static System Response for 569.5Ω Sensor
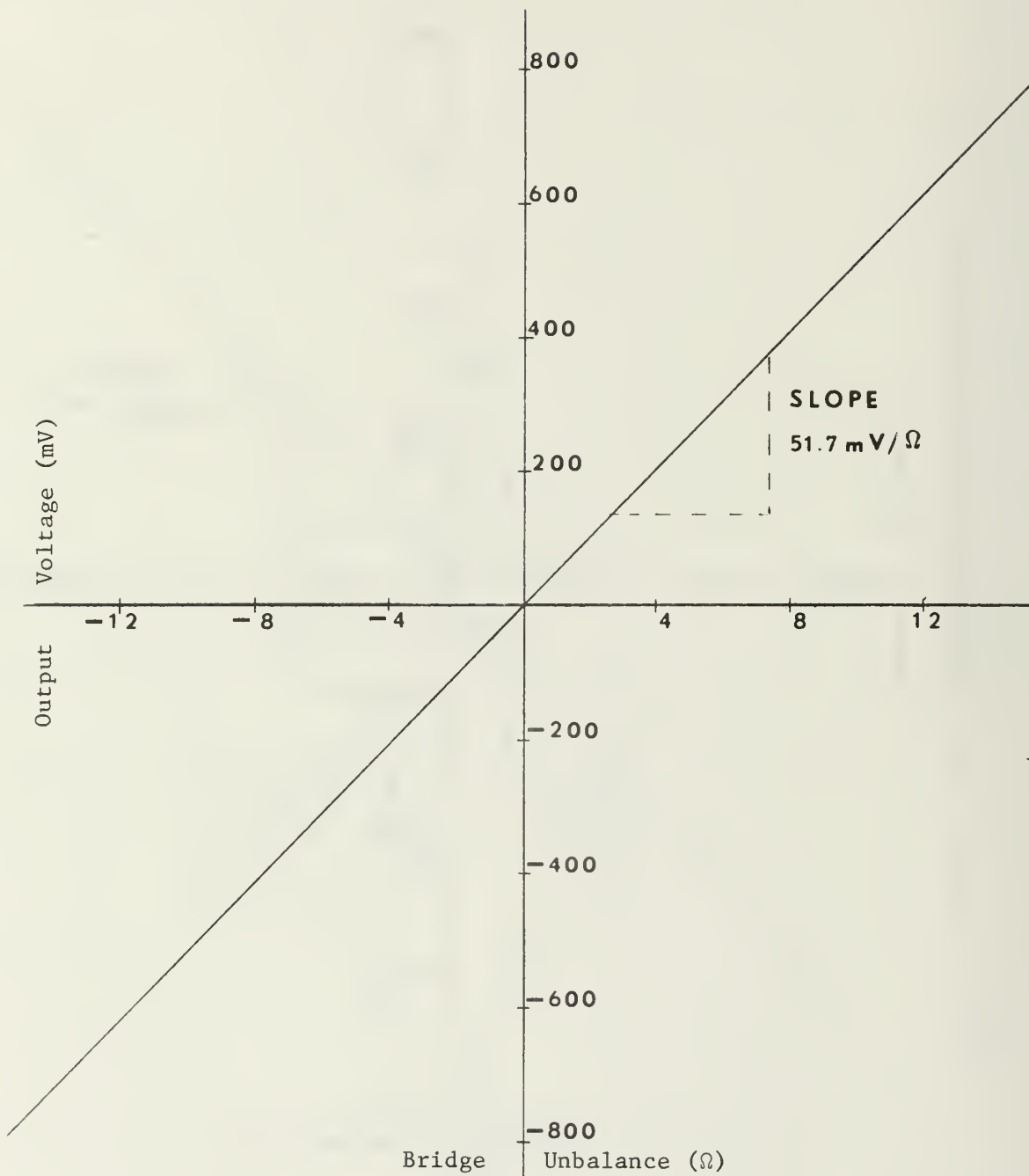
17

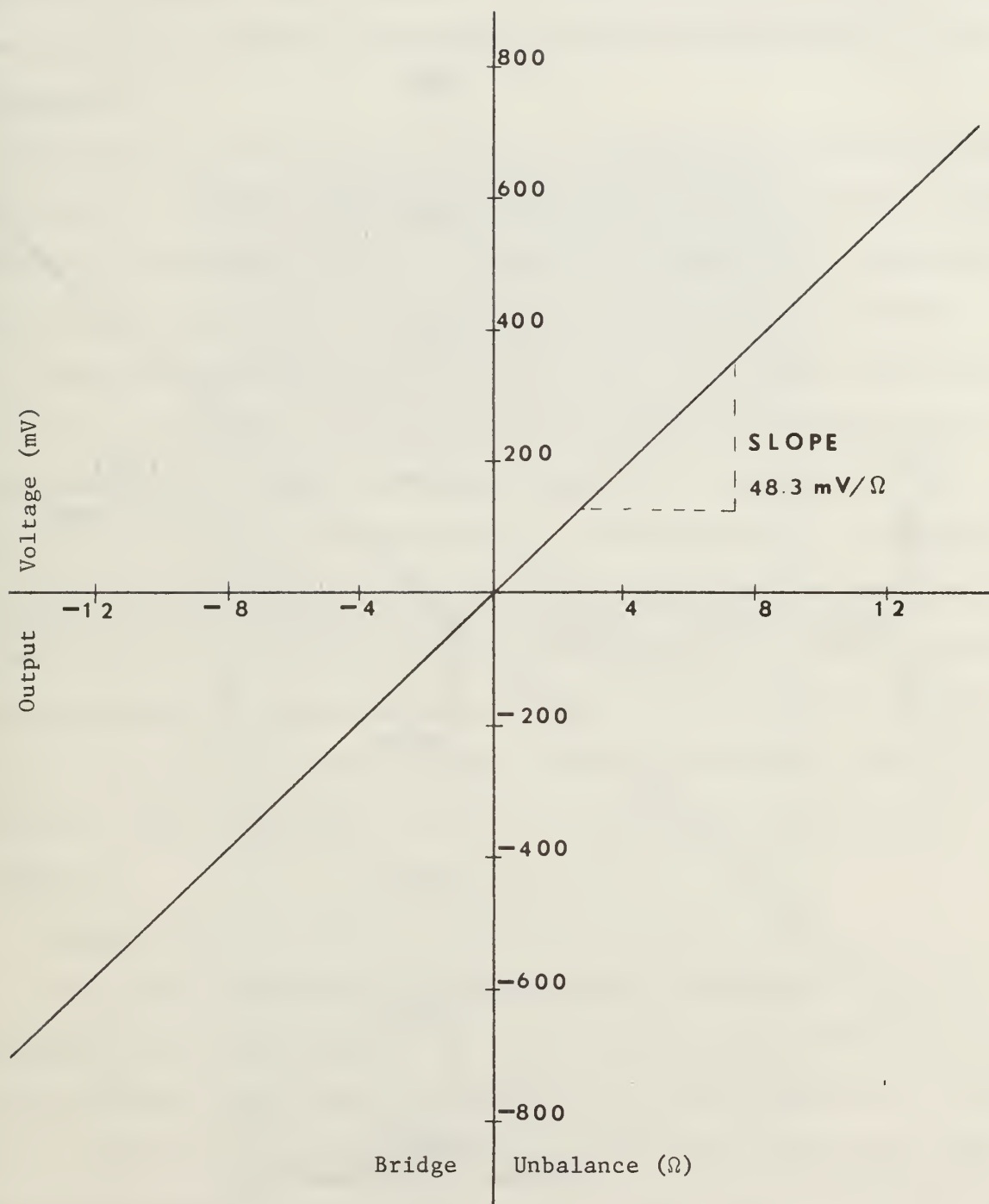Figure 7b . Static System Response for 662.5Ω Sensor

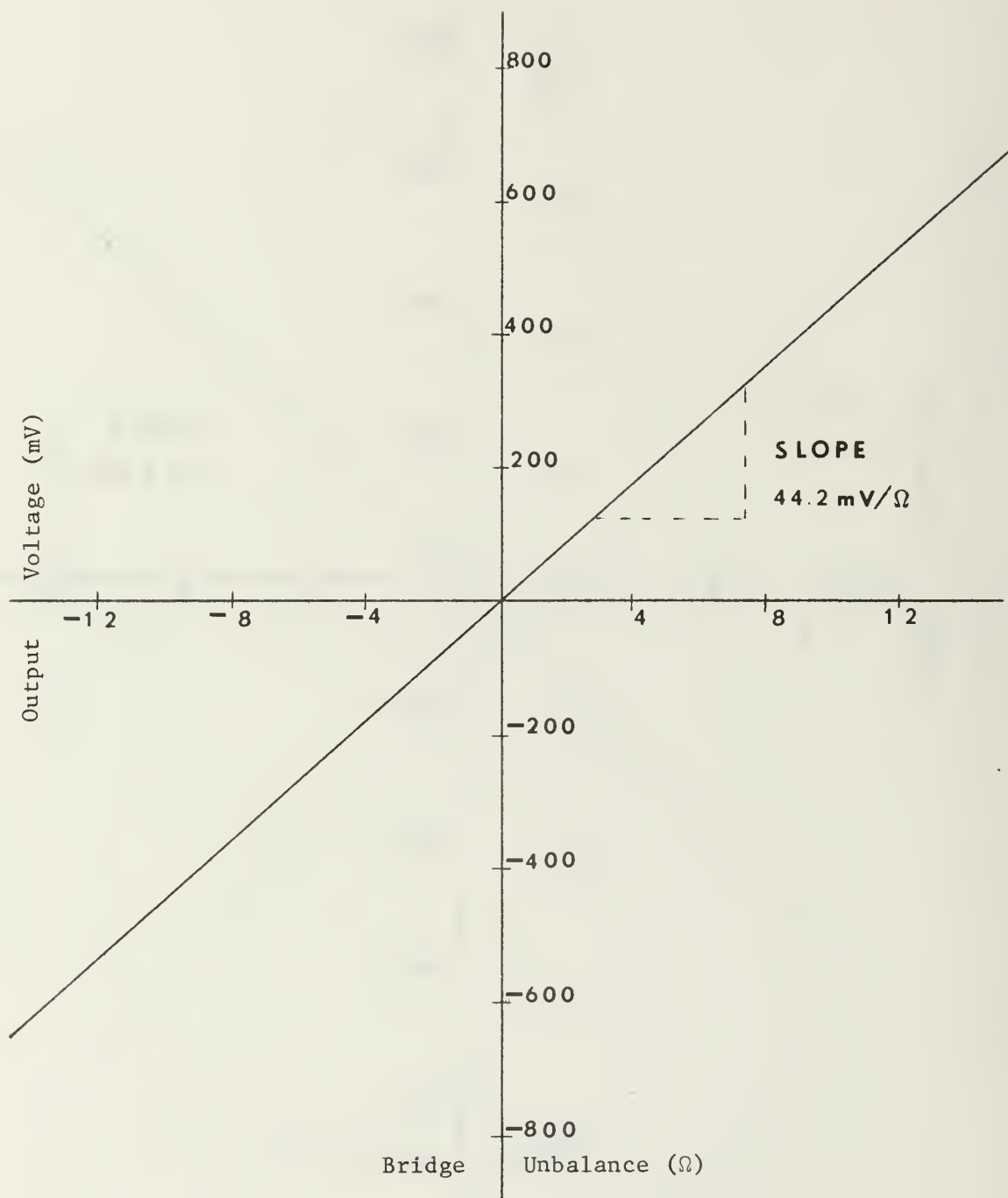Figure 7c. Static System Response for 789.0Ω Sensor

Figure 7d. Static System Response for 904.6Ω Sensor

although each temperature fluctuation sensed by the platinum wire is directly
proportional to output voltage variation, the constant of proportionality (slope,
indicated on plots in Figure 7) varies with the static resistance of the sensor.

4. Electronics

The electronic system described cannot be attributed to any single individual.
It was developed by National Electrolab Associates of Vancouver, British Columbia
in consultation with myself and Dr. M. Miyake of the Institute of Oceanography,
University of British Columbia. The first model was completed in 1968 and
three of the modified version described here in 1969. The overall system con-
sists of 1) a multivibrator circuit whose output is an 80 kHz square wave for
bridge excitation, 2) a balanceable bridge which serves as a modulator, 3) a
bridge circuit in which the platinum wire sensor forms one leg, 4) a differential
amplifier whose gain is fixed at 60 db, 5) a synchronous detector which demodu-
lates the carrier, 6) a low pass filter which minimizes high frequency components
in the output and 7) an operational amplifier with fixed incremental voltage
gains of 3, 5, 10 and 20. These components, with the exception of the sensor,
probe and its cable, are encased in a 2 in. by 6 in. x 8 in. metal chassis
box (Figure 8).

a. Multivibrator

Two 2N4124 transistors and their associated components form a sinu-
soidal 80 kHz multivibrator (Figure 9). The sinusoidal output drives a 2N4126
switching transistor which shapes a square wave of constant amplitude (0.2 mv peak
to peak). Oscilloscope inspection revealed some rounding of the leading edge
of the wave which suggests that harmonics of the 80 kHz signal are being attenuated.
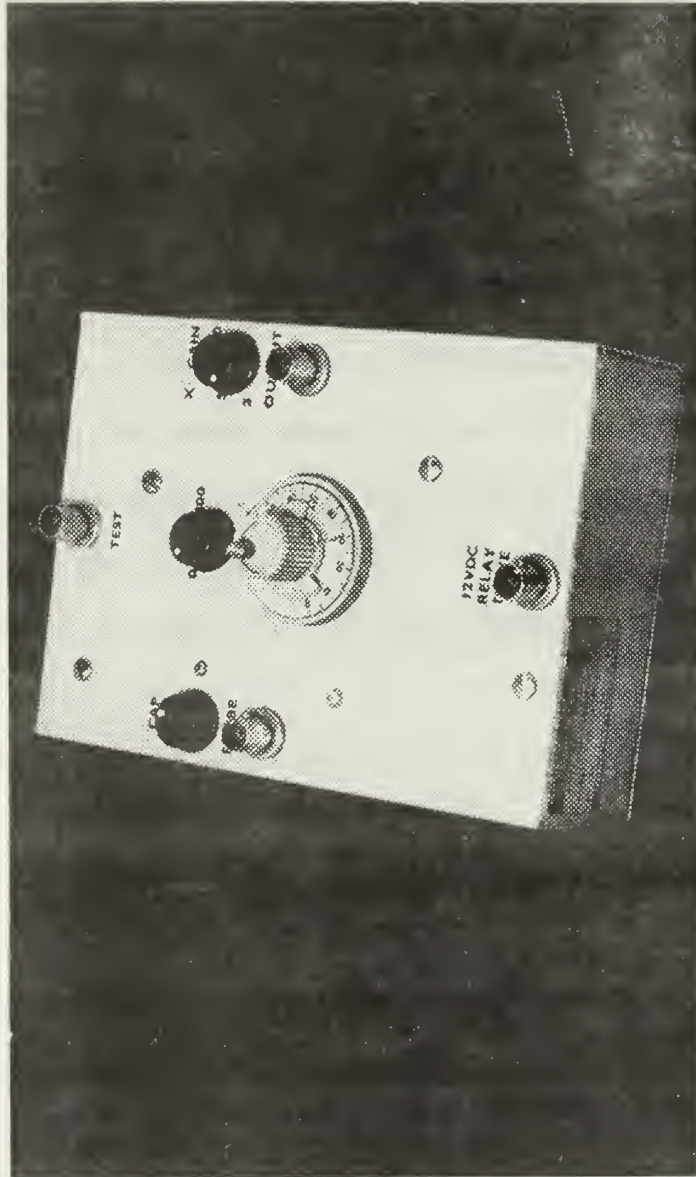
Figure 8. Metal Chassis Containing Temperature System.

Figure 9. Multivibrator Circuit.

23

b. Bridge amplifier

The bridge amplifier (Figure 6) is a differential amplifier with a fixed gain of 60 db. The circuit gain is set by the 10 KΩ and 10 Ω resistors in the feedback loop. The frequency compensation network composed of the 10 pf and 3 pf capacitors stabilize the integrated circuit for any amount of feedback. The circuit provides a relatively high gain small signal amplifier with excellent closed-loop frequency response. The gain was measured to be flat to 150 kHz and then begins to fall. This causes the leading edge of the 80 kHz square wave to be rounded slightly since harmonics of 80 kHz are attenuated.

c. Synchronous detector

The synchronous detector (Figure 10) recovers the amplified sensor signal. It consists of a coupling capacitor which passes the modulated square wave amplified by the bridge differential amplifier, an 80 kHz bandpass circuit formed by a 5 mh choke and a 700 pf capacitor which attenuates frequencies not near 80 kHz, a 2N422 FET which operates as a switch synchronized with the 80 kHz oscillator and a low pass filter which rejects the 80 kHz square wave and passes the signal frequency to the output amplifier.

The detector was noticed to cause slight low frequency distortion of the modulated carrier but no significant phase shift between the oscillator input to the detector and the carrier was observed.

d. DC amplifier

The DC (operational) amplifier (Figure 10) is a DC amplifier with feedback. The feedback can be changed incrementally to allow voltage gains of 3, 5, 10 and 20. The amplifier includes a frequency compensation network and has a closed-loop response which is flat beyond 100 kHz.

The measured frequency response of the operational amplifier was nearly flat (less than 1 db attenuation) to 10 kHz. Its gain for each gain selection
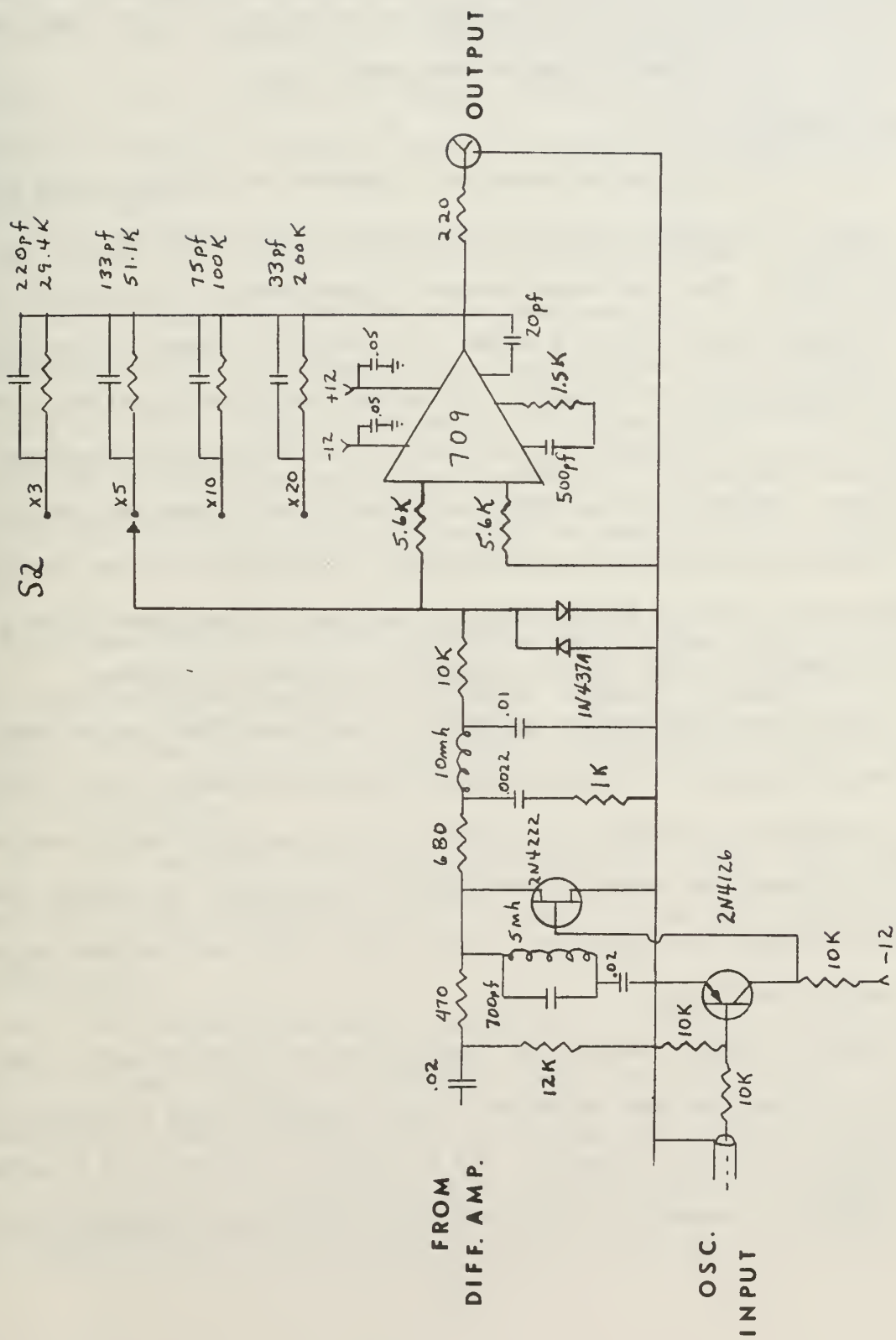
24

Figure 10. Synchronous Detector and Operational Amplifier.

was measured with a digital voltmeter to be correct to within ± 1 mv. A very low frequency drift of the output voltage was noted, which is neither surprising nor alarming in view of difficulties in stabilizing low frequency amplifiers. Another non-troublesome feature was oscillation of the output at 3.1 MHz when a gain of 3 was used. A bypass capacitor can prevent this.

5. System Operation

Any temperature fluctuation sensed by a platinum wire sensor causes a resistance change of the wire directly proportional to the magnitude of the temperature change. The resistance change is approximately 2.5Ω per 1C° for a 0.25μm platinum wire of length 0.30 mm. Any resistance change in one leg of a balanced bridge causes the bridge to become unbalanced and a portion of the excitation voltage to be applied to the input of the differential amplifier. Since the input impedance of the differential amplifier is high, the applied signal is directly proportional in magnitude to the magnitude of the unbalancing resistance and its polarity is determined by whether the resistance causing the unbalance is greater or less than the sensor's resistance at balance.

The input to the differential amplifier, a modulated 80kHz square wave, is amplified and coupled to the synchronous detector for demodulation. Since the time constant of the coupling components is much greater than the period of the 80kHz signal, the period of the signal is unaltered, the average level of the output becomes zero regardless of the input level, and the wave top acquires a small linear tilt.

The bandpass circuit, resonant at 80kHz, presents a high impedance path to ground for frequencies near 80kHz and a lower impedance path to ground for other frequencies which are unwanted. The circuit's Q, the ratio of resonant frequency (80kHz) to bandwidth (20kHz by manufacturer's specifications), is

low indicating that the impedance, a maximum at 80kHz, does not change rapidly with frequency. At frequencies in the vicinity of 15.9kHz the 700pf capacitor's impedance becomes quite large and the series resonant circuit formed by the 5mh choke and the .02μf capacitor becomes important, approximating a short to ground. As a result of this filtering, the 80kHz modulated signal should arrive at the field effect transistor relatively free of extraneous noise except in the band from 70kHz to 90kHz.

The 2N4222 field effect transistor, ultimately switched by the multivibrator via the 2N4126 transistor, functions as a phase-sensitive, half wave rectifier by presenting a very high impedance path to ground when not conducting and a very low path when conducting. Alternate half cycles of the 80kHz signal are passed to the lowpass filter or shorted to ground. This circuit which is synchronized with the multivibrator also senses the polarity of the selected half cycles.

The lowpass filter, unable to follow the rapid changes of the rectified 80kHz signal, recreates the wave shape which originally modulated the carrier and applies the wave form to the input of the operational amplifier for pre-selected amplification.

The output impedance of the operational amplifier (about 300Ω) permits the amplifier to be connected directly to most recording and display devices.

6. System Noise

Since the transient and spatial resolution requirements are adequately handled by the small sensor, the overall system noise level becomes the factor determining the minimum turbulence level (smallest temperature fluctuations) that can be measured. The general problem that has haunted the seeker of fine scale turbulence data is that the noise spectrum continues to be flat (constant

27

amplitude) at frequencies where the turbulence spectrum begins to decrease
rapidly. The unfortunate result is that of those scales at which much interest
may be centered, the noise level exceeds the turbulence signal level. This
same theme is presented here with only minor variations.

a. Measurement

The dummy probe (section 3b) was used to make measurements of rms noise
free of variations due to temperature fluctuations. A variable filter and rms
voltmeter were used. The noise of the filter and temperature system (Figure 11)
and then filter only was measured. The filter contributed less than 2% towards
the noise level at 1kHz. The most disturbing part of the noise spectrum is that
rather than being flat it increases with frequency particularly in the 1 to 2
kHz region. The noise at higher frequencies is less disturbing since these
frequencies are beyond the area of interest and can be filtered out. This aspect
is disappointing and will be considered in more detail.

b. Analysis

The noise at the input of the differential amplifier (bridge amplifier)
results primarily from the resistance noise (Johnson noise) of the bridge circuit
and the inherent noise of the amplifier. referred to the input.

The mean-square noise voltage across a resistor is proportional to bandwidth
(BW) and to the value of the resistor (R) or the equivalent resistance component
of impedance across which the noise is produced. For an assumed bandwidth of
10kHz and an approximate bridge impedance of 1000Ω, the noise level of the
bridge circuit was calculated according to (Terman, 1955),

$$e = \sqrt{4kTBR} \qquad\qquad (8)$$

where k is Boltzmann's constant and T is absolute temperature in °k. The noise
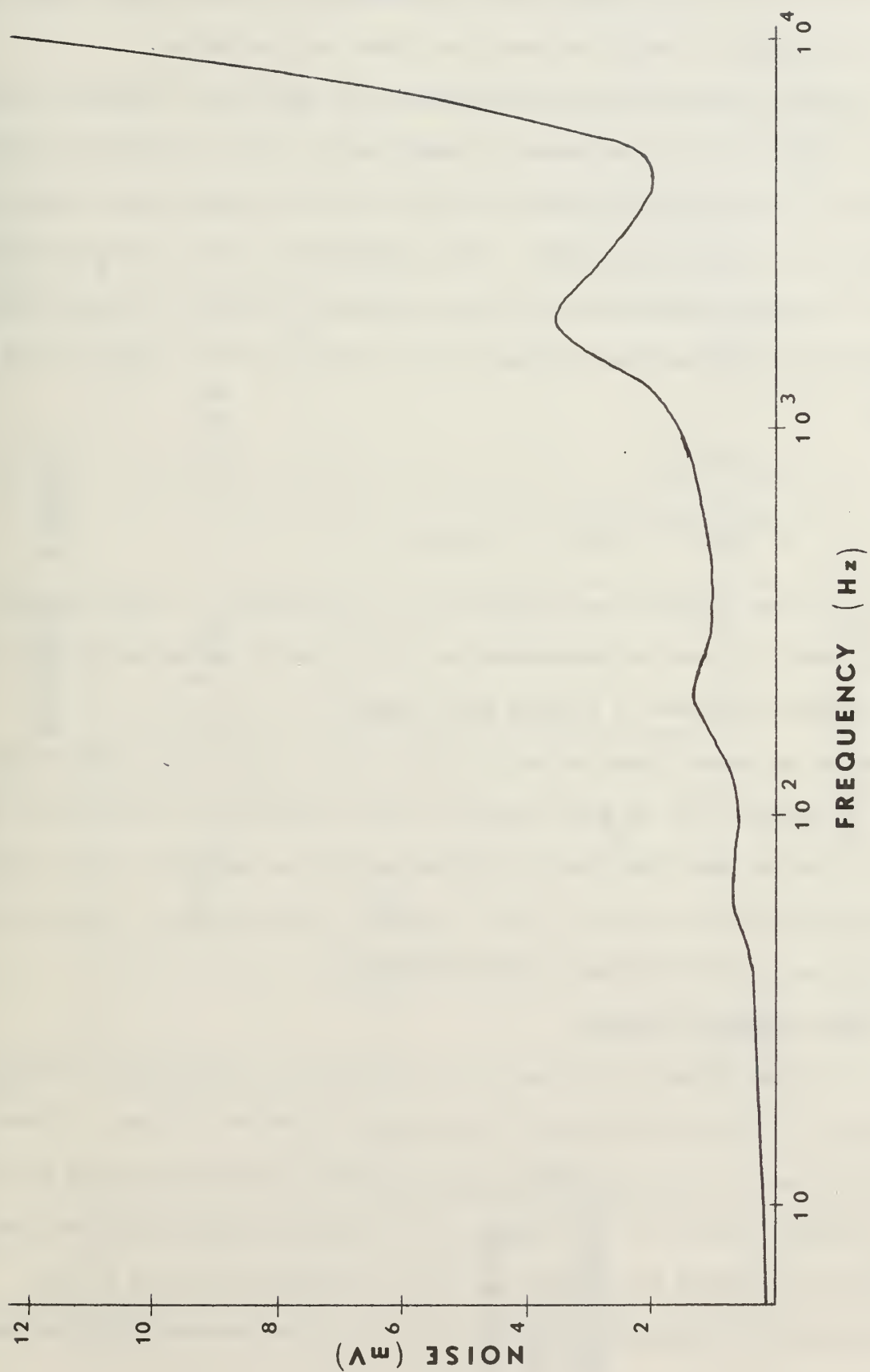level from the bridge circuit at room temperature was found to be 0.40μv rms.

28

Figure 11. Noise Level of System and Test Filter.

Peak noise which varies randomly will occassionally be much larger than 0.40μv but let us assume it rarely exceeds four times the rms value.

The broad band amplifier noise added by the amplifier, referred to the input for a 1000Ω source resistance is approximately 1.0μv rms (Fairchild Semiconductor, 709 integrated circuit). This value is 2.5 times larger than that calculated for the bridge circuit. The significance of this result increases when one considers that when two noise sources are combined, the noise power contributions add (rather than voltage) so that the equivalent input voltage (e_{ne}) becomes

$$e_n = \sqrt{e_n^2 + e^2} \qquad\qquad (9)$$

$$= \sqrt{(0.4)^2 + (1.0)^2} = 1.08\mu v \text{ rms}$$

where e_n is the bridge noise voltage and e is the amplifier noise voltage. Clearly there is room for improvement at this point by replacing the 709 integrated circuit with one of a lower noise figure.

Since the overall gain of the circuits which follow the bridge circuit is about 890 whenever the 3x gain position of the DC amplifier (section 4d) is used, the noise resulting from the bridge circuit and amplifier should generate an output of about 0.96 mv rms, which compares favourably with that measured over the lower part of the frequency range (Figure 11).

7. System Frequency Response

The system frequency response was determined by introducing a variation into one leg of the bridge circuit which modulated the 80 kHz carrier. A field effect transistor was used as a variable resistor with its value controlled by a signal generator (Figure 12). A square wave voltage was applied and the rise time measured. The signal was assumed to reach its maximum value in 3 time constants and the relation rise time equals 2.2 time constants (Millman and
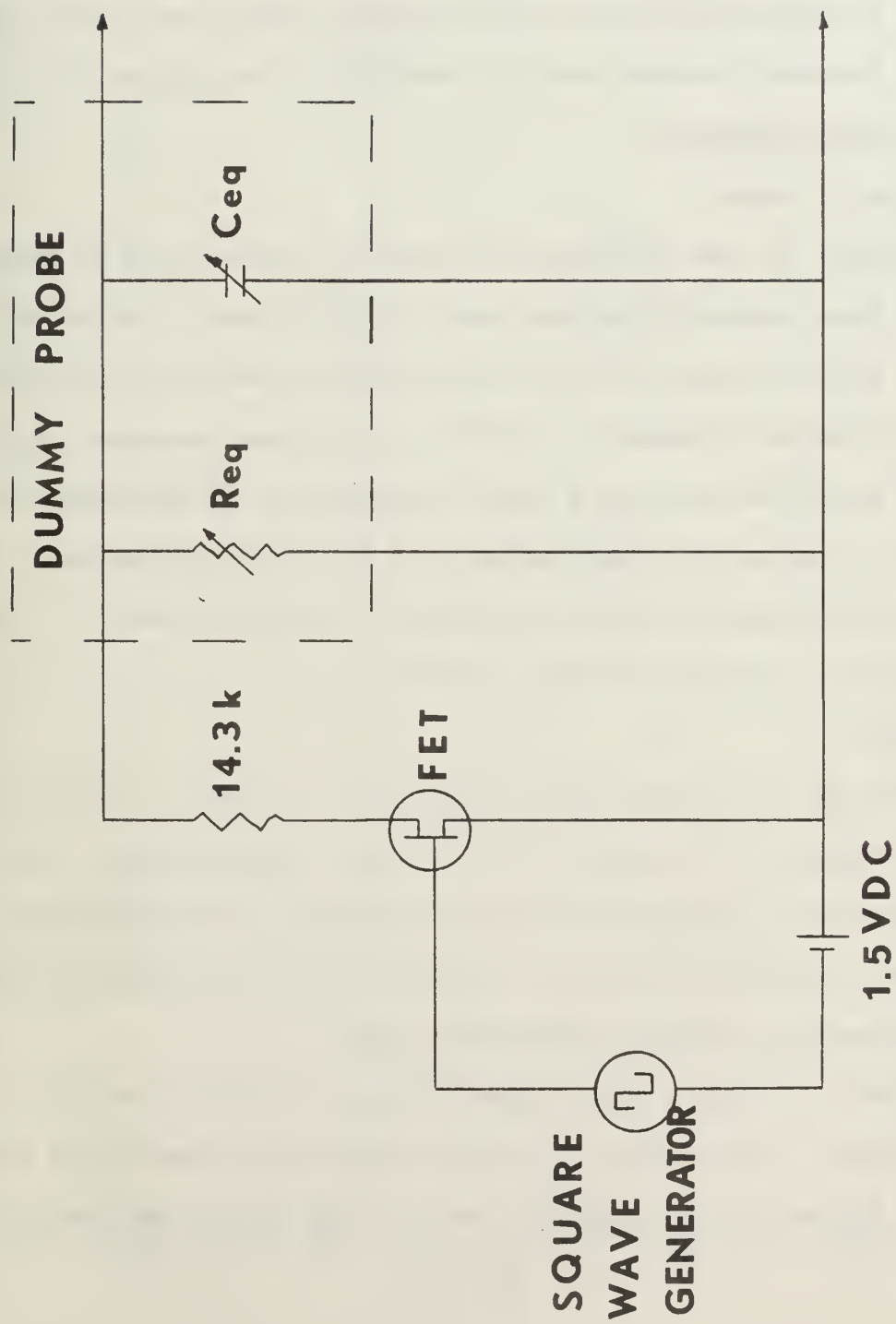
30

Figure 12. Frequency Response Circuit.

Taub, 1965 was used to calculate the system's time constant which governs the systems frequency response.

The system frequency response test primarily reflects the response of the detector circuit. The modulated carrier observed at the output of the differential (bridge) amplifier was free of distortion but after coupling to the detector slight low frequency distortion of the modulated carrier was noted. The overall system frequency response was flat from DC to 5 kHz (Figure 13).

8. Examples of Data Collected

a. Temperature signal

An example of some temperature fluctuation data is given in Figure 14. The top record shows reasonably uniform levels of turbulence. The second record shows a signal that is tending to be one-sided although small scale fluctuations remain uniformly active throughout. The third record shows a signal exhibiting both quiet and active sections and a shape characteristic of atmospheric temperature signals - - a gradually rising leading edge and sharp trailing edge. The bottom record shows another intermittent signal. Further discussion of these data can be found in a report by Boston (1973b).

b. Spectra

Because of the extremely fast response of the sensor, the temperature signal was recorded not only directly but also after differentiation. This latter procedure was to increase the temperature signal at high frequencies relative to low frequencies. It may be correctly considered as prewhitening the rapidly decreasing high frequency temperature signal.

The spectrum of a typical direct signal (Figure 15a) shows the -5/3 (inertial subrange) slope expected of turbulent atmospheric temperature fluctuations at these frequencies but fails to show the shape of the spectrum at frequencies
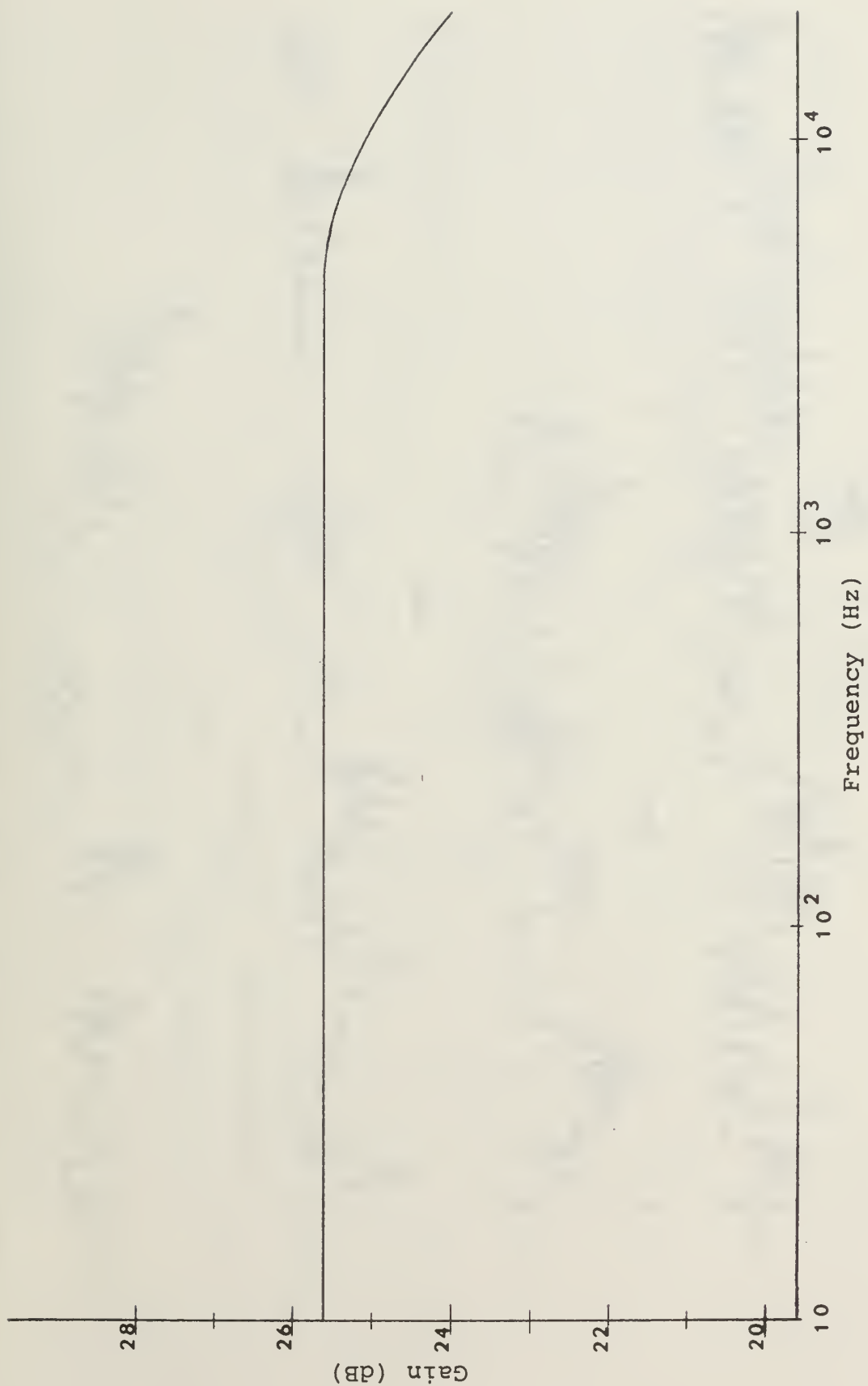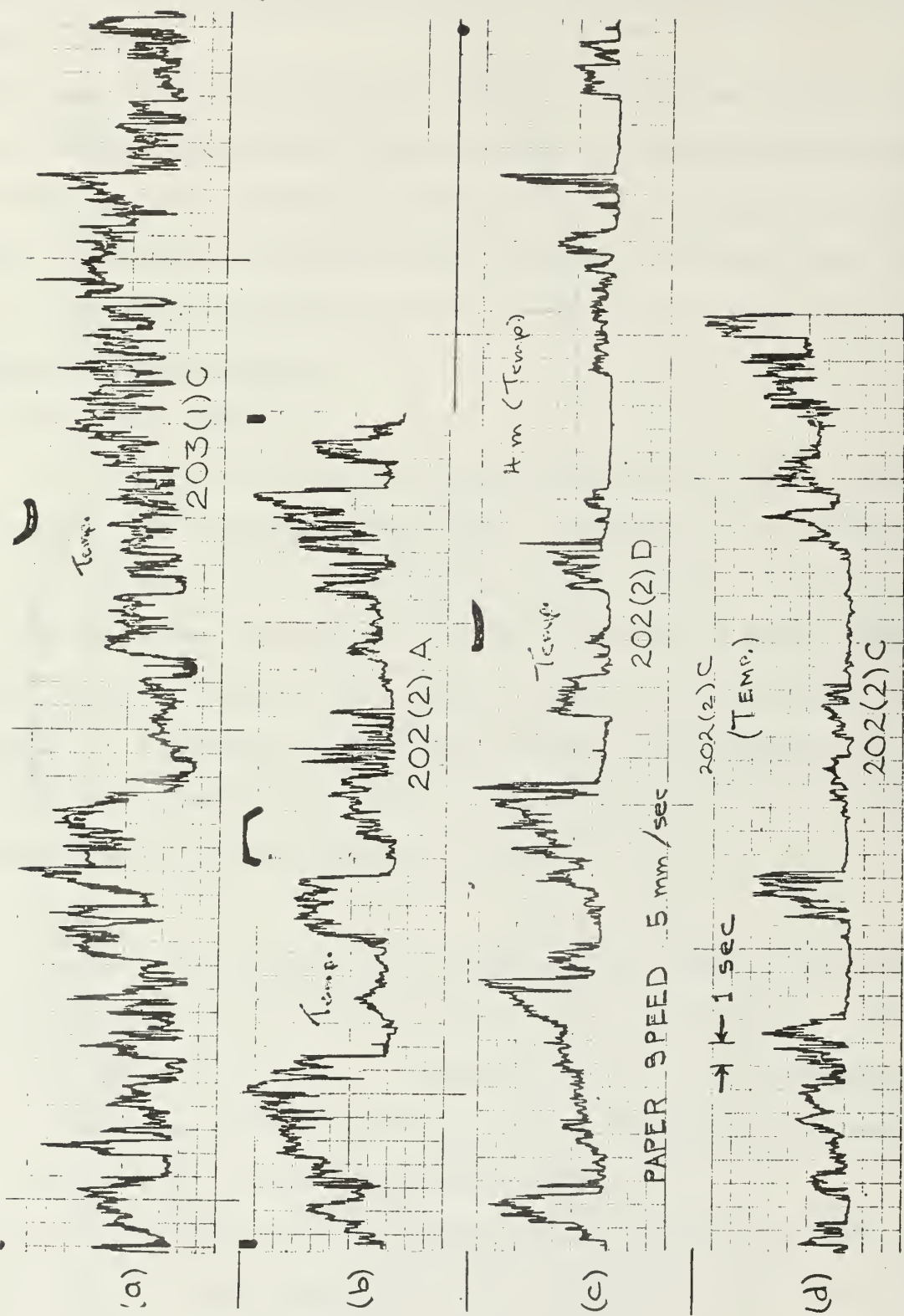
Figure 13. System Frequency Response.

33

Figure 14. Temperature Fluctuation Time Series.

34
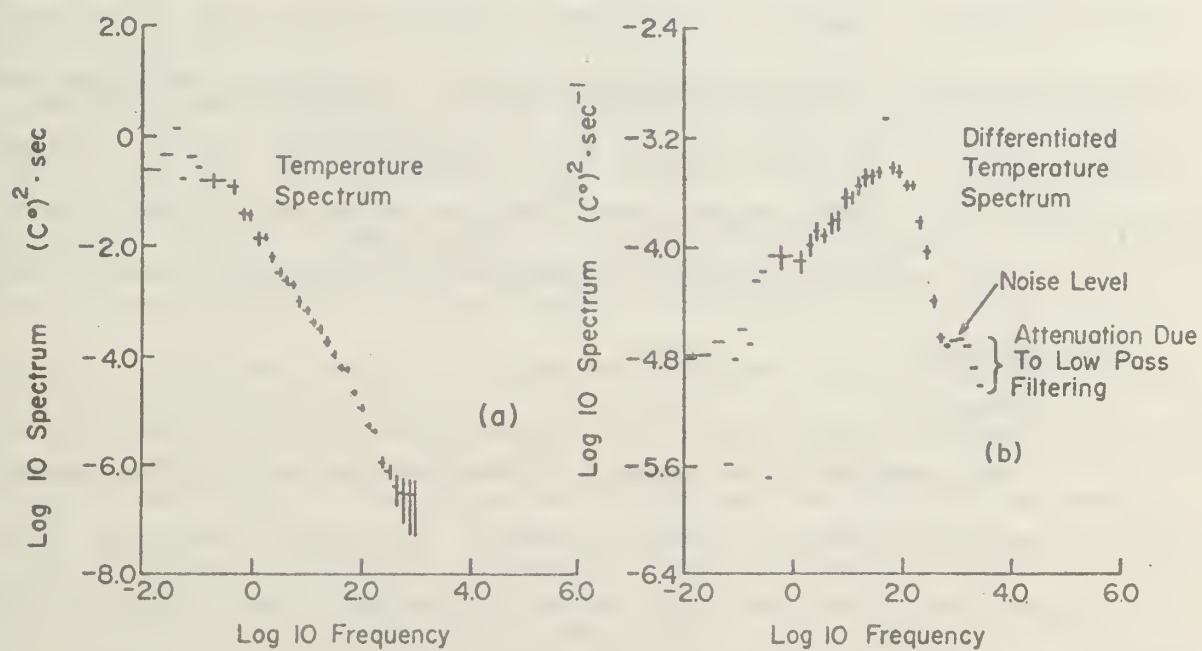
Figure 15. Spectra of Temperature Fluctuations.

beyond 100 Hz. This disappointing result is primarily because the noise level of the temperature electronics system is not low enough at frequencies above 100 Hz. Clearly other sources of noise exist such as those encountered in filtering, pre-whitening, recording and analysis. However the main source is the noise contained in the original signal.

The differentiated spectrum now becomes of paramount importance. It shows (Figure 15b) the "inertial subrange" shape (which appears as +1/3 for a differentiated turbulence signal), the peak where maximum dissipation of temperature fluctuations occur and the dissipation region. In addition the noise level is clearly defined as is the effect of the low pass filter. This is decidedly an encouraging result which demonstrates that the system may be used effectively to study high frequency atmospheric temperature fluctuations (Boston, 1972).

9. Conclusions

a. Sensor

The practicality of using a 0.25µm diameter wire in the atmosphere may be questioned and justly so. Hinze (1959, p. 94) states that 2.5µm is considered a practical lower limit for the diameter of platinum wires although 0.625µm wires have since been used successfully by Gibson et al (1970) for example. Extensive experience now has been obtained with 0.25µm diameter wires in a variety of conditions. One wire was used over a desert (near Richland, Washington) for 6 hours in winds ranging from 4 to 7 m/sec. At this same site, on a separate occasion, another wire remained intact for over an hour in a sand storm with winds of 12 m/sec. These wires also have been used successfully to measure temperature fluctuations over the ocean (at the Spanish Banks field site operated by the Institute of Oceanography University of British Columbia). At this location a single wire has lasted for several days. Over a tidal mud flat (Boston, 1972)

36

no breakages were encountered once the probe was mounted on the mast. It appears

then, that a properly constructed wire of these dimensions may be operated under

the same conditions that a 2.5μm hot wire would be expected to operate. However,

the 0.25μm wire compares unfavorably to hot wires in that it is very susceptible

to breakage by jarring or knocking. Extreme caution must be exerted not only in

mounting such probes but also in ensuring that no jarring of the support occurs

after mounting.

   b.   Electronics

       Whereas the electronics has no frequency response problem there does

appear to be some room for improvement with respect to noise. It is not clear

that the substitution of a dummy resistor for the thin wire leads to a valid noise

test. Analyses were made of quiescent sections of temperature fluctuation data

(Section 6a). The signal levels of these sections were all consistent and lower

than the noise level for the dummy sensor. The noise figures then may be too high.

Even so, the noise level of the system is marginal and improvements are needed.

These could be made in the present system for example by means of improved

amplifiers in place of the bridge and DC amplifiers. Other methods are being

investigated. The ideal system has still not been achieved and its development

remains an honourable goal.

Acknowledgements

References

Boston, N.E.J. 1970 An investigation of high-wavenumber temperature and velocity spectra in air. Ph.d. thesis, University of British Columbia.

Boston, N.E.J. and Burling, R.W. 1972 An investigation of high-wave number temperature and velocity spectra in air. J. Fluid Mech. 55 473.

Boston, N.E.J. 1973a. Some statistics of high-wavenumber temperature and velocity fluctuations in the atmospheric boundary layer. Tech. Rept. Naval Postgraduate School.

Boston, N.E.J. 1973b Temperature fluctuations in the atmospheric boundary layer. Tech. Rept. Naval Postgraduate School.

Chao, Y. and Sandborn, R.V. 1964 Characteristics of fine wire platinum resistance thermometer. Tech. Rept. Colorado State University.

Fabula, A.G. 1962 The plume test method of determining the dynamic response of towed thermometers. Tech. Rept. 62-3, Pacific Naval Laboratory, Esquimalt, Canada.

Flow Corporation Bulletin No. 25. 1956 Hot wire anemometry. Flow Corporation, Watertown, Massachusetts.

Gibson, C.H., Stegen, G.R. and Williams, R.B. 1970 Statistics of the fine structure of turbulent and temperature fields measured at high Reynolds number. J. Fluid Mech. 41, 153.

King, L.V., 1914 On the convection of heat from small cylinders in a stream of fluid. Phil. Trans. Ruy. Soc., London, A214, 373.

Krechmer, S. I. 1954 Methods of measurements of micropulsations of the wind velocity and temperature in the atmosphere. Trudy Geofix. Inst. ANUSSR, 24, 43

Hinze, J.O. 1959 Turbulence. McGraw-Hill

Millman, J. and Taub, H. 1965 Pulse, Digital and Switching Waveforms. McGraw-Hill

Wyngaard, J.C. 1971 The effect of velocity sensitivity on temperature derivative statistics. J. Fluid Mech. 53, 317

INITIAL DISTRIBUTION LIST

No. Copies

1. Defense Documentation Center   2
    Cameron Station
    Alexandria, Virginia 22314

2. Library, Code 0212   2
    Naval Postgraduate School
    Monterey, California 93940

3. Dean of Research, Code 023   1
    Naval Postgraduate School
    Monterey, California 93940

4. Dr. Michel Coantic   1
    Institut de Mecanique Statistique
    de la Turbulence
    12, Avenue General Leclerc
    Marseille (3^e), France

5. Dr. Niels Busch   1
    Research Establishment Riso
    DK-4000 Roskilde, Denmark

6. Dr. M. Donelin   1
    Canada Centre for Inland Waters
    867 Lakeshore Road
    Postal Box 5050
    Burlington, Ontario
    Canada

7. Commander, Naval Undersea Center   1
    Attn: Dr. A. G. Fabula
    San Diego, California 92132

8. Dr. Carl Friehe   1
    University of California, San Diego
    Department of AMES
    P.O. Box 109
    La Jolla, California 92037

9. Dr. Carl Gibson   1
    University of California, San Diego
    Department of AMES
    P.O. Box 109
    La Jolla, California 92037

10. Dr. H. L. Grant   1
    Defense Research Establishment Pacific
    Esquimalt, British Columbia
    Canada

11.   Dr. A. Gyr   1
       Institute of Hydromechanics and
       Water Resources Management
       8006 Zurich, Tannenstrasse 1
       Switzerland

12.   Dr. David Halpern   1
       Pacific Oceanographic Laboratories
       University of Washington, WB-10
       Seattle, Washington 98105

13.   Mr. F. E. Jerome   1
       Physics Department
       Malaspina College
       Nahaimo, British Columbia
       Canada

14.   Dr. J. C. Kaimal   1
       AFCRL (LYB)
       L. G. Hanscom Field
       Bedford, Massachusetts 01730·

15.   Dr. A. D. Kirwin, Jr.   1
       Department of Oceanography
       School of Geosciences
       Texas A and M University
       College Station, Texas

16.   Dr. Søren Larson   1
       Research Establishment Risø
       DK-4000 Roskilde, Denmark

17.   Dr. D. M. McEligot   1
       Energy, Mass and Momentum Transfer Laboratory
       Aerospace and Mechanical Engineering Department
       The University of Arizona
       Tucson, Arizona 85721

18.   Dr. M. Miyake   1
       Institute of Oceanography
       University of British Columbia
       Vancouver 8, British Columbia
       Canada

19.   Dr. E. Mollo-Christensen   1
       Dept. Of Meteorology
       Massachusetts Institute of Technology
       Cambridge, Massachusetts

No. Copies

20. Dr. James J. O'Brien   1
     Program Director
     Physical Oceanography
     Ocean Science and Technology Division
     Office of Naval Research
     Arlington, Virginia 22217

21. Dr. Clayton Paulson   1
     School of Oceanography
     Oregon State University
     Corvallis, Oregon 97331

22. Dr. S. D. Smith   1
     Atlantic Oceanographic Laboratory (DEMR)
     Bedford Institute
     Dartmouth, Nova Scotia
     Canada

23. Dr. R. W. Stewart, Director   1
     Marine Sciences Branch, Pacific Region
     Department of the Environment (Federal)
     1230 Government Street, 5th Floor
     Victoria, British Columbia
     Canada

24. Paul Twitchell   1
     Office of Naval Research
     495 Summer Street
     Boston, Massachusetts 02210

25. Dr. C. W. Van Atta   1
     Department of Earth Sciences
     University of California
     La Jolla, California

26. Dr. R. M. Williams   1
     Oregon State University
     School of Oceanography
     Corvalles, Oregon 97331

27. Dr. J. R. Wilson   1
     Wave Climatology Study
     Marine Sciences Branch
     Dept. of Environment
     615 Booth Street
     Ottawa, Canads K1A-OE6

28. Dr. J. Wyngaard   1
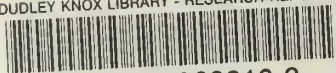   AFCRL (LYB)
     L. G. Hanscom Field
     Bedford, Massachusetts 01730

No. Copies

29. Department of Oceanography   6
     Naval Postgraduate School
     Monterey, California 93940

30. Oceanographer of the Navy   1
     Hoffman II
     200 Stovall Street
     Alexandria, Virginia 22332

31. Naval Oceanographic Office   1
     Library (Code 3330)
     Washington, D. C. 20373

32. Director of Defense Research and Engineering   1
     Office of the Secretary of Defense
     Washington, D. C. 20301
     ATTN: Office, Assistant Director (Research)

33. Office of Naval Research   5
     Department of the Navy
     Arlington, Virginia 22217
     3 ATTN: Ocean Science & Technology Division (Code 480)
     1 ATTN: Naval Applications & Analysis Division
                 (Code 460)
     1 ATTN: Earth Sciences Division (Code 417)

34. Director   12
     6 ATTN: Library, Code 2029 (ONRL)
     6 ATTN: Library, Code 2000

35. Commander   2
     Naval Oceanographic Office
     Washington, D. C. 20390
     1 ATTN: Code 1640 (Library)
     1 ATTN: Code 70

36. Director   1
     National Oceanic and Atmospheric Administration
     National Oceanographic Data Center
     Washington Navy Yard
     Rockville, Maryland 20852

37. Dr. Noel Boston   6
     Department of Oceanography
     Naval Postgraduate School
     Monterey, California 93940